

Experimental and Modeling Study of the Oxidation of Benzaldehyde

S. Namysl¹, L. Pratali², M. Pelucchi², O. Herbinet¹, A. Stagni², T. Faravelli², F. Battin-Leclerc^{*,1}

¹Laboratoire Réactions et Génie des Procédés, CNRS-Université de Lorraine, 1 rue Grandville, 54000 Nancy, France

²Department of Chemistry, Materials and Chemical Engineering "G. Natta", Politecnico di Milano, P.zza Leonardo da Vinci 32, 20133 Milano, Italy

Abstract

The gas-phase oxidation of benzaldehyde has been investigated in a jet-stirred reactor. Benzaldehyde is an aromatic aldehyde commonly considered in bio-oils surrogates or in the oxidation of fuels such as toluene. However, its oxidation has never been previously investigated experimentally and no product formation profiles were reported in the few pyrolysis studies. In this study 48 species, mainly CO, CO₂ and phenol were detected using gas chromatography, which indicate a rapid formation of phenyl radicals. This was confirmed by a kinetic analysis performed using the current version of the CRECK kinetic model, in which reactions have been updated.

Introduction

Benzaldehyde is the lightest aromatic aldehyde and is one of the major intermediates in the combustion and atmospheric oxidation of benzyl radical [1]. For this reason, its formation and consumption are accounted for in detailed kinetic models for the combustion of toluene and heavier aromatic compounds (e.g. [2–4]). Furthermore, many oxygenated aromatic compounds are formed during the decomposition of biomass [5,6] and aromatic aldehydes (e.g. furfural and derivatives or hydro-benzaldehydes and methoxy-benzaldehyde (see Fig. 1)) are a non-negligible part of these products [5,6].

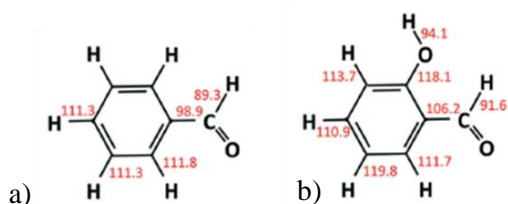


Fig. 1. Structures of a) benzaldehyde, b) hydroxyl-benzaldehyde. Bond dissociation energies of molecules are given at 298K and in kcal mol⁻¹[7]

Generally, oxygenated aromatic compounds (phenol, anisole, catechol, guaiacol, vanillin) are gaining academic and industrial interest due to their presence in bio-oils from biomass fast pyrolysis [2,8,7]. Therefore, the influence of different functional groups on their combustion properties should be systematically addressed. Moreover their impact on PAHs and soot growth should be better analyzed, as the high aromatic content of bio-oils could lead to undesired increased formation of particulate matter.

The purpose of this study is then to understand the decomposition of benzaldehyde, the lightest aromatic aldehyde under oxidizing conditions.

Benzaldehyde pyrolysis had already been studied in batch reactors by Hurd and Bennet [9] and by Solly and

Benson [10] covering a temperature range from 573K to 963K at atmospheric pressure. Experiments with this reaction have also been carried out in flow reactors by Grela et al. [11] at high temperatures (1005-1270K) and low-pressure (P=0.001atm), by Bruinsma et al. [12] at atmospheric pressure and over a temperature range from 773K to 1173K, and by Vasiliou et al. [13] between 1200K and 1800K and between 0.1 and 0.2 kPa. These studies showed that benzaldehyde decomposes to give phenyl radical plus H atom and CO:

$C_6H_5CHO (+M) \rightarrow C_6H_5CO + H \rightarrow C_6H_5 + CO + H$,
contrary to the usual aliphatic aldehydes where the alkyl acyl bond is the weakest (R-CHO). However none of these studies provided mole fraction profiles for the fuel or the decomposition products for benzaldehyde pyrolysis. Also to our knowledge no oxidation study has been performed.

The aim of this study is to propose a first set of data for the oxidation of benzaldehyde in a jet-stirred reactor (JSR) coupled with gas chromatographs (GC). Using different type of detectors, mole fractions profiles were obtained for benzaldehyde and 48 of its products. Then these profiles were used to update the benzaldehyde oxidation subset in the current version (1902) of the CRECK kinetic model.

Experimental methods

The JSR used for the experiments has already often been used for kinetic studies of pyrolysis [14] and combustion [15]. It consists of a fused silica sphere (volume 92 cm³) equipped with four injection nozzles positioned in a cross located at the center of the sphere. This injection method ensures high turbulences in the reactor and leads to homogeneity in both product concentration and gas phase temperature thanks to a quartz annular preheating zone preceding the reactor inlet, in which the temperature of the gas is increased up to the reactor temperature.

*Corresponding author: frederique.battin-leclerc@univ-lorraine.fr
Proceedings of the European Combustion Meeting 2019

Table 1

Reactions added or modified in order to account for the chemistry of benzaldehyde oxidation.

Reaction	<i>A</i>	<i>n</i>	<i>E_a</i>	References	No.
Reactions of Benzaldehyde					
Unimolecular initiation					
$C_6H_5CHO=HCO+C_6H_5$	$5.00E+15$	0.0	98900.0	CRECK	(1)
$C_6H_5CHO=C_6H_5CO+H$	$3.00E+15$	$0,0$	$89300,0$	CRECK	(2)
$C_6H_5CO=>C_6H_5+CO$	$5.80E+14$	0.0	23000.0	[16]	(3)
Bimolecular initiations and H-abstractions					
$O_2+C_6H_5CHO=HO_2+C_6H_5CO$	$1.36E+07$	2.0	41405.9	CRECK	(4)
$OH+C_6H_5CHO=H_2O+C_6H_5CO$	$1.20E+10$	1.0	-855.1	CRECK	(5)
$HO_2+C_6H_5CHO=H_2O_2+C_6H_5CO$	$3.20E+06$	2.0	14062.9	Estimated	(6)
$CH_3+C_6H_5CHO=CH_4+C_6H_5CO$	$2.40E+05$	2.0	3516.3	CRECK	(7)
$H+C_6H_5CHO=H_2+C_6H_5CO$	$1.20E+07$	2.0	2573.6	Estimated	(8)
$C_6H_5CHO+C_7H_7=C_7H_8+C_6H_5CO$	$1.08E+05$	2.0	14062.9	CRECK	(9)
$C_2H_5+C_6H_5CHO=C_2H_6+C_6H_5CO$	$1.60E+05$	2.0	5128.0	CRECK	(10)
$C_6H_5+C_6H_5CHO=C_6H_6+C_6H_5CO$	$2.96E+08$	1.0	867.9	CRECK	(11)
$C_5H_5+C_6H_5CHO=C_5H_6+C_6H_5CO$	$2.72E+05$	2.0	12129.8	CRECK	(12)
$C_6H_5CHO+C_6H_5O=C_6H_5OH+C_6H_5CO$	$1.44E+05$	2.0	10683.4	[7]	(13)
Ipsso-additions					
$C_6H_5CHO+O=C_6H_5O+HCO$	$4.00E+12$	0.0	5000.0	[17]	(14)
$C_6H_5CHO+CH_3=C_7H_8+HCO$	$1.50E+12$	0.0	4000.0	[7]	(15)
$C_6H_5CHO+C_2H_3=C_6H_5C_2H_3+HCO$	$1.20E+12$	0.0	15200.0	[7]	(16)
$C_6H_5CHO+OH=C_6H_5OH+HCO$	$9.63E+13$	0.0	19228.0	[7]	(17)
$C_6H_5CHO+H=C_6H_6+HCO$	$4.70E+12$	0.0	8600.0	[7]	(18)

The gas residence time inside the annular preheater is very short compared to its residence time inside the reactor (a few percent) to limit the reactivity in this section. The heating is ensured by resistances (Thermocoax) rolled around the reactor and the preheating zone, which allows flexibility and swiftness in the heating of each area. Temperatures are measured by K-type thermocouples located inside the inlet cross and between the resistances and the external wall of the reactor. The reaction temperature is assumed to be equal to that measured in the inlet cross according to the isothermal reactor hypothesis, with a gradient of $\pm 5K$.

Benzaldehyde was provided by Sigma Aldrich with a purity of 99%. He (99.999% pure) and O₂ (99.999%) were provided by Messer. Gas flow rates are controlled by mass flow controllers and the liquid flow rate by a Coriolis flow controller followed by a vaporization chamber maintained 10 K above benzaldehyde boiling temperature. The relative uncertainty in the flow measurements is around 0.5% for each controller, thus about 2% on the residence time.

The outlet gas leaving the reactor is then transported by a heated line to GCs. The first GC, equipped with a Carbosphere packed column, a thermal conductivity detector (TCD) and a flame ionization detector (FID), is used for the quantification of light-weight compounds

like methane, ethylene, acetylene and ethane. The second GC is fitted with a Q-Bond capillary column and a FID, preceded by a methanizer, is used for the quantification of compounds containing from 2 carbon atoms, like acetylene or ethylene to compounds with 5 carbon atoms (e.g. cyclopentadiene). The methanizer (nickel catalyst for hydrogenation) makes it possible to detect species like CO and CH₂O with a good sensitivity. A third GC equipped with a HP-5 capillary column is used for the detection of the heaviest compounds. Products like benzene, benzaldehyde, phenol, naphthalene or biphenyl are quantified on this apparatus. The identification of reaction products is performed using a GC equipped with both types of capillary columns and coupled to a mass spectrometer (quadrupole). Calibrations are performed by injecting standards when it is possible with a maximum relative error in mole fractions around $\pm 5\%$ and $\pm 10\%$ for the other species calibrated using the effective carbon number method.

Description of the kinetic model

The kinetic subset of benzaldehyde in the global CRECK model was updated. The reactions modified or added in the mechanism are listed in Table 1.

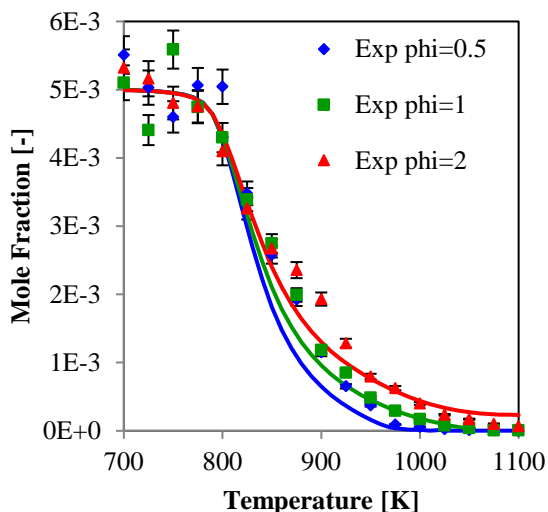


Fig. 2. Comparison between experimental (symbols) and predicted (lines) mole fraction profiles of benzaldehyde

The OpenSMOKE++ package [18] has been used to perform all the kinetic simulations and analyses here presented. The CRECK mechanism has been recently updated with a new core mechanism for C_0 - C_3 species from Metcalfe et al. [19] and from Burke et al. [20], as well as for the heavier compounds from Ranzi et al [21,22]. The rate constant of reaction (3) has been estimated from that proposed by Simmie et al. [16], but with an activation energy increased by 6 kcal/mol, to account for resonance stabilization of the carbonyl radical. Rate constants for ipso-additions reactions have been taken according to the work of Pelucchi et al. [7] except the one with oxygen atom which was taken from the work of Saggese et al. [17]. The pre-exponential factors of reactions (6) and (8) have also been modified by a factor of 0.5 and 0.3 respectively. The kinetic values were already present in the mechanism and were reduced in order to reproduce the fuel reactivity in the error range estimated for those parameters.

Results and discussion

Benzaldehyde oxidation was studied between 700K and 1100K at 107 kPa at three equivalence ratios: $\phi=0.5$ -1-2. The residence time in the reactor was fixed at 2 s and the inlet mole fraction of fuel was 0.5%. Helium was used as the inert gas.

Fig. 2 presents the mole fraction profile of benzaldehyde between 700K and 1100K with an associated experimental error of 5%. Benzaldehyde starts typically to react at 750K and is fully consumed at 1025K except for fuel rich conditions. It can be also observed that the equivalence ratio has only a minor impact on the conversion of the fuel. Figure 4 displays the mole fraction profiles of the main products obtained during the oxidation of benzaldehyde.

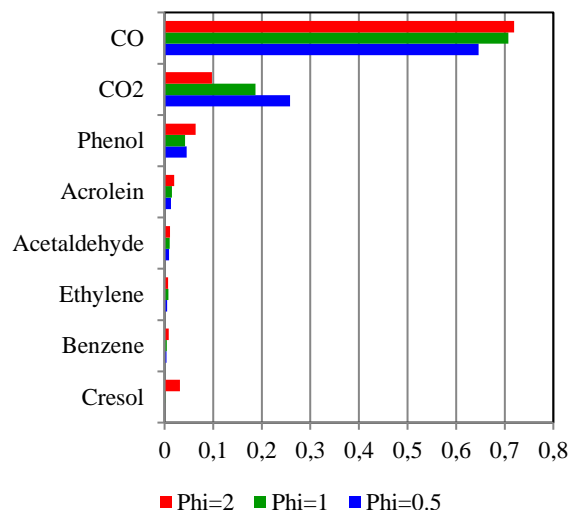


Fig. 3. Selectivity analysis at 850K for the three equivalence ratios.

48 products have been identified during this study; they can be divided in three main categories:

- Linear compounds: carbon monoxide, carbon dioxide, methane, acetylene, ethylene, ethane, propene, propyne, acetaldehyde, acrolein, acetone, allene, butenyne, butadiene.
- Cyclic oxygenated compounds: cyclopentenone, anisole, benzoquinone, phenol, benzofuran, benzodioxol, hydroxybenzaldehyde, cresol, acetophenone, benzodioxol-2-one, methylbenzofuran, ethylphenol, cinnamaldehyde, diphenylether, dibenzofuran, indanone.
- Cyclic hydrocarbons: 1.3-cyclopentadiene, benzene, toluene, ethylbenzene, xylene, phenylacetylene, styrene, cumene, methylstyrene, indene, methylindene, dihydronaphthalene, naphthalene, biphenyl, acenaphthylene.

Due to our analytical set-up, the quantification of hydrogen and water is not possible. It can also be noticed that formaldehyde or catechol were not detected during the experiments. Those products could have been expected due to the presence of phenol and methane in the gas phase with oxygen. Fig. 3 presents the product selectivity at 850K for stoichiometric conditions. It shows that carbon monoxide and carbon dioxide are the main products at this temperature. Phenol, acrolein, acetaldehyde and ethylene are the other main products formed. Cresol is a specific product of the fuel rich conditions. For each condition a carbon mass balance has been calculated and is estimated to be around 90% of the global inlet of carbon atoms. The overall agreement between the experimental and modeling data presented in Fig. 2 and 4 is acceptable especially for equivalence ratios of 0.5 and 1. The fuel consumption is well described but the model exhibits a higher dependence to the equivalence ratio than that experimentally measured.

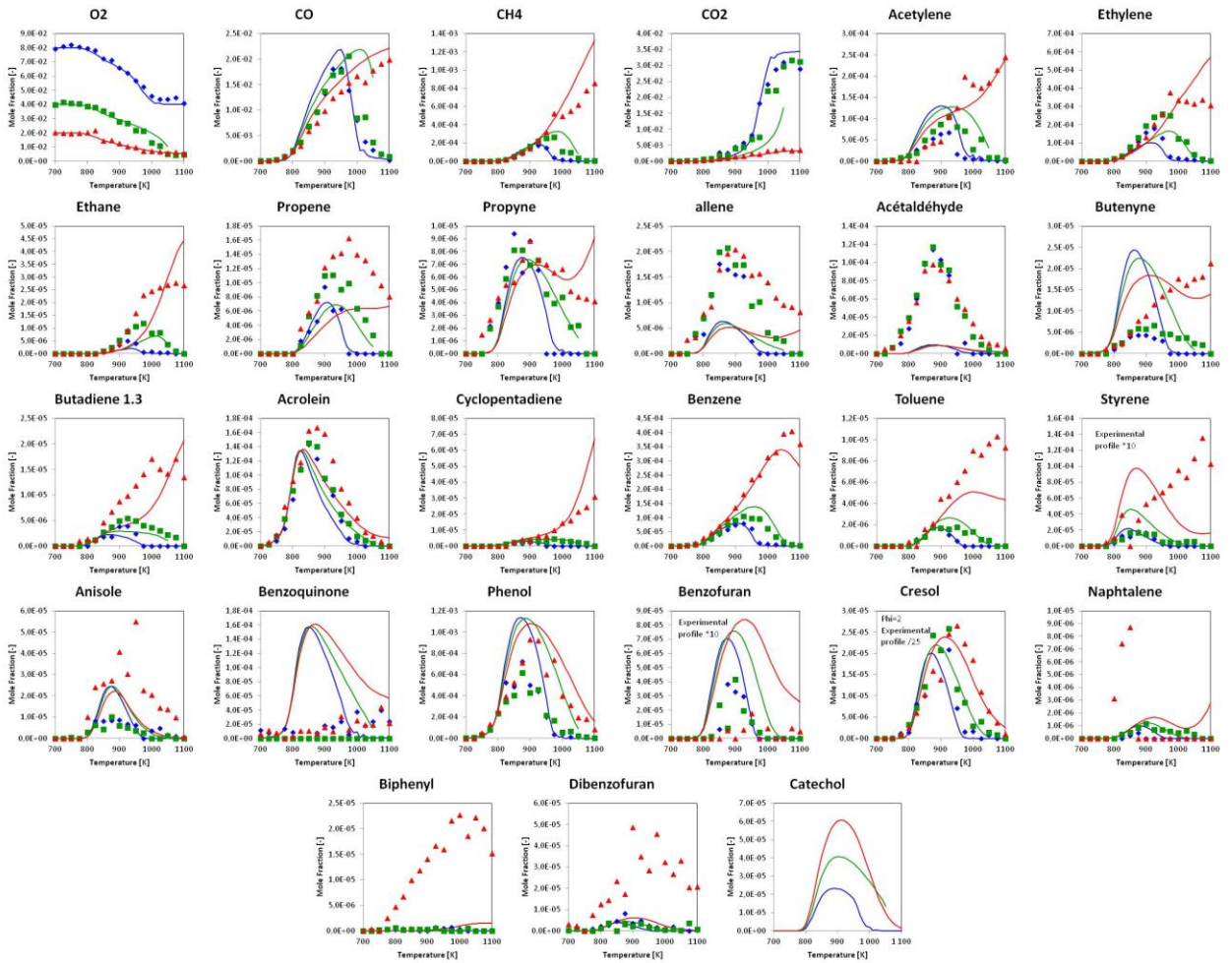


Fig. 4. Benzaldehyde oxidation in a jet-stirred reactor at $\phi=0.1, 1$ and 2 , $p=107$ kPa and $\tau=2.0$ s. Comparison between experimental (symbols: $\blacklozenge=\phi=0.5$, $\blacksquare=\phi=1$, $\blacktriangle=\phi=2$) and predicted (lines) mole fractions of major species.

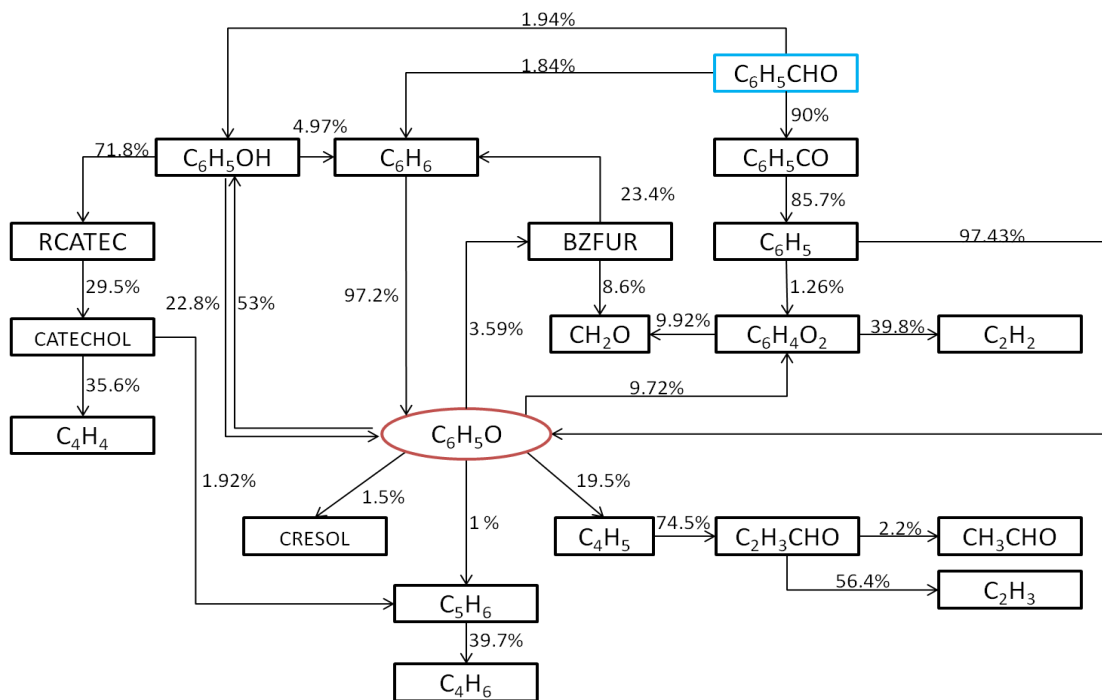


Fig. 5. Rate of production analysis at 850 K and 107 kPa of benzaldehyde oxidation under stoichiometric conditions

At the highest temperature ($T > 1000\text{K}$) for fuel rich conditions, model predictions are less accurate. The model predicts a consumption of benzene and toluene higher than that experimentally observed, which leads to an overprediction of 1,3-cyclopentadiene, ethane, propyne and methane. The model also does not predict as much acetaldehyde as experimentally measured and estimates a production of catechol which was not observed experimentally. The profile of benzoquinone ($\text{C}_6\text{H}_4\text{O}_2$) is also overpredicted by the model.

Numerical solutions were not found for stoichiometric conditions above 1050K . The model predicts a transient behavior contrary to experiments, in which a stable behavior was observed.

Fig. 5 shows a rate flux analysis of benzaldehyde oxidation in terms of carbon atom at 850K for stoichiometric conditions. For more clarity, some species like CO and CO_2 are not shown. Under these conditions benzaldehyde mainly decomposes by the abstractions of the aldehydic hydrogen atom as suggested by Vasiliou et al. [13] for pyrolysis. Benzaldehyde also reacts by ipso-addition reactions of hydrogen atom and OH radical producing benzene and phenol. The main decomposition pathway leads to the formation of the $\text{C}_6\text{H}_5\text{CO}$ radical, which quickly decomposes by alpha-scission in phenyl radical and carbon monoxide. The phenyl radical then leads to phenoxy radical. This radical is the precursor of almost all the product experimentally observed. Benzene is also almost exclusively transformed into $\text{C}_6\text{H}_5\text{O}$ via two pathways:

- $\text{O} + \text{C}_6\text{H}_6 = \text{H} + \text{C}_6\text{H}_5\text{O}$
- $\text{R} + \text{C}_6\text{H}_6 = \text{RH} + \text{C}_6\text{H}_5$; $\text{C}_6\text{H}_5 + \text{O}_2 = \text{C}_6\text{H}_5\text{O} + \text{O}$

$\text{C}_6\text{H}_5\text{O}$ is also produced by phenol, one of the main products.

As discussed in [17], the resonance stabilized phenoxy radical largely contributes to phenol formation by means of H-abstraction ($\text{C}_6\text{H}_5\text{O} + \text{RH} = \text{C}_6\text{H}_5\text{OH} + \text{R}$) and recombination with H atoms. But phenol reacts with radical, such as O , OH , HO_2 , ..., to give $\text{C}_6\text{H}_5\text{O}$ radicals again. So a cycle phenol/phenoxy is exhibited by the mechanism and could be important in the reactivity of the $\text{C}_6\text{H}_5\text{O}$ radical.

Acetaldehyde and acrolein are produced by the decomposition of $\text{C}_6\text{H}_5\text{O}$ to C_4H_5 and CO through the reaction: $\text{O} + \text{C}_6\text{H}_5\text{O} \Rightarrow 2\text{CO} + \text{C}_4\text{H}_5$. Then the C_4H_5 radical reacts with oxygen to form HCO and acrolein: $\text{O}_2 + \text{C}_4\text{H}_5 \Rightarrow \text{HCO} + \text{C}_2\text{H}_3\text{CHO}$. Acrolein leads to the formation of mainly C_2H_3 radicals and acetaldehyde. To form C_2H_3 radicals $\text{C}_2\text{H}_3\text{CHO}$ reacts with different radicals (OH , O , H) to give C_2H_3 , CO : $\text{R} + \text{C}_2\text{H}_3\text{CHO} \Rightarrow \text{RH} + \text{CO} + \text{C}_2\text{H}_3$. The lumped step corresponds to the abstraction of the aldehydic H-atom followed by an alpha-scission of the acyl bond ($\text{R}-\text{C}^*=\text{O}$). Acetaldehyde is formed by the reaction: $\text{OH} + \text{C}_2\text{H}_3\text{CHO} \Rightarrow \text{HCO} + \text{CH}_3\text{CHO}$. However the model is not able to predict the correct amount of acetaldehyde

and the transformation of acrolein into acetaldehyde needs a better assessment.

Conclusion

Benzaldehyde oxidation has been investigated for the first time. Using a JSR coupled with gas chromatographs, 48 compounds have been identified for various equivalence ratios covering the fuel lean to rich conditions. 28 mole fraction profiles have been obtained for species from major ones (CO , CO_2 , phenol) to some minor products (acrolein, acetaldehyde, benzene, cresol...). These new data were compared with simulation results obtained with an updated version of the CRECK kinetic model. The model update allowed for a better description of benzaldehyde oxidation. The decomposition of benzaldehyde mainly leads to the formation of phenyl radicals which then oxidize to give $\text{C}_6\text{H}_5\text{O}$ radical, which is the radical at the origin of almost all the observed products. Another relevant reaction class is that of ipso-addition reactions leading to the formation of benzene and phenol. Those compounds also react to give $\text{C}_6\text{H}_5\text{O}$ radical. The model succeeds to reproduce almost all the mole fraction profile. However it does not succeed to estimate correctly the observed amount of acetaldehyde.

This work confirms the importance of the $\text{C}_6\text{H}_5\text{O}$ radical in the decomposition of oxygenated aromatic compounds and provides a first detailed assessment of benzaldehyde oxidation kinetics.

Acknowledgements

This work has received funding from the European Union H2020 (H2020-SPIRE-04-2016) under grant agreement n°723706 and from the COST Action CM1404 "Chemistry of smart energy carriers and technologies".

References

- [1] N. Sebbar, J.W. Bozzelli, H. Bockhorn, Thermochemistry and Reaction Paths in the Oxidation Reaction of Benzoyl Radical: $\text{C}_6\text{H}_5\text{C}^*(=\text{O})$, *J. Phys. Chem. A.* 115 (2011) 11897–11914. doi:10.1021/jp2078067.
- [2] W. Pejpichestakul, E. Ranzi, M. Pelucchi, A. Frassoldati, A. Cuoci, A. Parente, T. Faravelli, Examination of a soot model in premixed laminar flames at fuel-rich conditions, *Proc. Combust. Inst.* (2018). doi:10.1016/j.proci.2018.06.104.
- [3] M. Pelucchi, C. Cavallotti, T. Faravelli, S.J. Klippenstein, H-Abstraction reactions by OH , HO_2 , O , O_2 and benzyl radical addition to O_2 and their implications for kinetic modelling of toluene oxidation, *Phys. Chem. Chem. Phys.* 20 (2018) 10607–10627. doi:10.1039/C7CP07779C.
- [4] B. Husson, M. Ferrari, O. Herbinet, S.S. Ahmed, P.-A. Glaude, F. Battin-Leclerc, New experimental evidence and modeling study of the ethylbenzene oxidation, *Proc. Combust. Inst.* 34 (2013) 325–333. doi:10.1016/j.proci.2012.06.002.

- [5] M. Bertero, G. de la Puente, U. Sedran, Fuels from bio-oils: Bio-oil production from different residual sources, characterization and thermal conditioning, *Fuel*. 95 (2012) 263–271. doi:10.1016/j.fuel.2011.08.041.
- [6] L. Negahdar, A. Gonzalez-Quiroga, D. Otyuskaya, H.E. Toraman, L. Liu, J.T.B.H. Jastrzebski, K.M. Van Geem, G.B. Marin, J.W. Thybaut, B.M. Weckhuysen, Characterization and Comparison of Fast Pyrolysis Bio-oils from Pinewood, Rapeseed Cake, and Wheat Straw Using ¹³C NMR and Comprehensive GC × GC, *ACS Sustain. Chem. Eng.* 4 (2016) 4974–4985. doi:10.1021/acsschemeng.6b01329.
- [7] M. Pelucchi, C. Cavallotti, A. Cuoci, T. Faravelli, A. Frassoldati, E. Ranzi, Detailed kinetics of substituted phenolic species in pyrolysis bio-oils, *React. Chem. Eng.* 4 (2019) 490–506. doi:10.1039/C8RE00198G.
- [8] M. Nowakowska, O. Herbinet, A. Dufour, P.-A. Glaude, Detailed kinetic study of anisole pyrolysis and oxidation to understand tar formation during biomass combustion and gasification, *Combust. Flame*. 161 (2014) 1474–1488. doi:10.1016/j.combustflame.2013.11.024.
- [9] C.D. Hurd, C.W. Bennett, The pyrolysis of benzaldehyde and of benzyl benzoate, *J. Am. Chem. Soc.* 51 (1929) 1197–1201. doi:10.1021/ja01379a030.
- [10] R. Solly, S. Benson, Kinetics of Gas-Phase Unimolecular Decomposition of Benzoyl Radical, *J. Am. Chem. Soc.* 93 (1971) 2127-. doi:10.1021/ja00738a006.
- [11] M. Grela, A. Colussi, Kinetics and Mechanism of the Thermal-Decomposition of Unsaturated Aldehydes - Benzaldehyde, 2-Butenal, and 2-Furaldehyde, *J. Phys. Chem.* 90 (1986) 434–437. doi:10.1021/j100275a016.
- [12] O.S.L. Bruinsma, R.S. Geertsma, P. Bank, J.A. Moulijn, Gas phase pyrolysis of coal-related aromatic compounds in a coiled tube flow reactor: 1. Benzene and derivatives, *Fuel*. 67 (1988) 327–333. doi:10.1016/0016-2361(88)90314-6.
- [13] A.K. Vasilioy, J.H. Kim, T.K. Ormond, K.M. Piech, K.N. Urness, A.M. Scheer, D.J. Robichaud, C. Mukarakate, M.R. Nimlos, J.W. Daily, Q. Guan, H.-H. Carstensen, G.B. Ellison, Biomass pyrolysis: Thermal decomposition mechanisms of furfural and benzaldehyde, *J. Chem. Phys.* 139 (2013) 104310. doi:10.1063/1.4819788.
- [14] N. Vin, O. Herbinet, F. Battin-Leclerc, Diethyl ether pyrolysis study in a jet-stirred reactor, *J. Anal. Appl. Pyrolysis*. 121 (2016) 173–176. doi:10.1016/j.jaap.2016.07.018.
- [15] O. Herbinet, F. Battin-Leclerc, Progress in Understanding Low-Temperature Organic Compound Oxidation Using a Jet-Stirred Reactor, *Int. J. Chem. Kinet.* 46 (2014) 619–639. doi:10.1002/kin.20871.
- [16] J.M. Simmie, Kinetics and Thermochemistry of 2,5-Dimethyltetrahydrofuran and Related Oxolanes: Next Next-Generation Biofuels, *J. Phys. Chem. A*. 116 (2012) 4528–4538. doi:10.1021/jp301870w.
- [17] C. Saggese, A. Frassoldati, A. Cuoci, T. Faravelli, E. Ranzi, A wide range kinetic modeling study of pyrolysis and oxidation of benzene, *Combust. Flame*. 160 (2013) 1168–1190. doi:10.1016/j.combustflame.2013.02.013.
- [18] A. Cuoci, A. Frassoldati, T. Faravelli, E. Ranzi, OpenSMOKE++: An object-oriented framework for the numerical modeling of reactive systems with detailed kinetic mechanisms, *Comput. Phys. Commun.* 192 (2015) 237–264. doi:10.1016/j.cpc.2015.02.014.
- [19] W.K. Metcalfe, S.M. Burke, S.S. Ahmed, H.J. Curran, A hierarchical and comparative kinetic modeling study of C1– C2 hydrocarbon and oxygenated fuels, *Int. J. Chem. Kinet.* 45 (2013) 638–675.
- [20] S.M. Burke, U. Burke, R. Mc Donagh, O. Mathieu, I. Osorio, C. Keesee, A. Morones, E.L. Petersen, W. Wang, T.A. DeVerter, M.A. Oehlschlaeger, B. Rhodes, R.K. Hanson, D.F. Davidson, B.W. Weber, C.-J. Sung, J. Santner, Y. Ju, F.M. Haas, F.L. Dryer, E.N. Volkov, E.J.K. Nilsson, A.A. Konnov, M. Alrefae, F. Khaled, A. Farooq, P. Dirrenberger, P.-A. Glaude, F. Battin-Leclerc, H.J. Curran, An experimental and modeling study of propene oxidation. Part 2: Ignition delay time and flame speed measurements, *Combust. Flame*. 162 (2015) 296–314. doi:10.1016/j.combustflame.2014.07.032.
- [21] E. Ranzi, A. Frassoldati, R. Grana, A. Cuoci, T. Faravelli, A. Kelley, C. Law, Hierarchical and comparative kinetic modeling of laminar flame speeds of hydrocarbon and oxygenated fuels, *Prog. Energy Combust. Sci.* 38 (2012) 468–501.
- [22] E. Ranzi, A. Frassoldati, A. Stagni, M. Pelucchi, A. Cuoci, T. Faravelli, Reduced Kinetic Schemes of Complex Reaction Systems: Fossil and Biomass-Derived Transportation Fuels, *Int. J. Chem. Kinet.* 46 (2014) 512–542. doi:10.1002/kin.20867.